Geophysical Research Letters

RESEARCH LETTER
10.1029/2024GL109339

Modeling Climate and Tectonic Controls on Bias in Measured River Incision Rates

Clarke DeLisle[1] and Brian J. Yanites[1]

[1]Department of Earth and Atmospheric Sciences, Indiana University, Bloomington, IN, USA

Key Points:

- We present a numerical model that reproduces biases in rates of river incision measured from strath terraces
- We find that these measurement biases are the strongest when climates are highly variable and rock uplift is slow
- Understanding bedrock incision measurement biases allows for bias correction in field studies and improves data comparability

Correspondence to:

B. J. Yanites,
byanites@iu.edu

Citation:

DeLisle, C., & Yanites, B. J. (2024). Modeling climate and tectonic controls on bias in measured river incision rates. *Geophysical Research Letters*, *51*, e2024GL109339. https://doi.org/10.1029/2024GL109339

Received 14 APR 2024
Accepted 27 AUG 2024

Author Contributions:

Conceptualization: Clarke DeLisle, Brian J. Yanites
Formal analysis: Clarke DeLisle, Brian J. Yanites
Funding acquisition: Brian J. Yanites
Methodology: Clarke DeLisle
Project administration: Brian J. Yanites
Software: Clarke DeLisle
Supervision: Brian J. Yanites
Visualization: Clarke DeLisle
Writing – original draft: Clarke DeLisle
Writing – review & editing: Brian J. Yanites

Abstract Rates of land surface processes provide insights into climatic and tectonic influences on topography. Bedrock incision rates are estimated by dating perched landforms such as strath terraces, assuming a constant bedrock incision rate from terrace abandonment to the next terrace level or present river level. These estimates express biases from the stochastic nature of sediment and water discharge in controlling river incision as well as from using a mobile channel elevation as a reference frame, leading to different incision rates when calculated over different timeframes. We introduce a 1-D model incorporating fluvial mechanics, tectonics, sediment, and climate variability to predict these biases and assess their sensitivity to climate and tectonics. Findings suggest biases intensify under highly variable climates and slow rock uplift, with climate periodicity being a primary control for our modeled scenarios. Our model provides a mechanism to improve river incision measurement uncertainty, impacting paleoclimate and tectonic geomorphology reconstructions.

Plain Language Summary Geomorphologists often measure how fast rivers erode bedrock over time by dating river terraces that have been uplifted to be higher than the elevation of the modern river channel. This helps us learn how landscapes evolve and about what past climates were like over long timescales. But this method is complicated by the fact that rivers do not erode rocks at a steady rate and the elevation of the channel surface above which we measure terrace height changes over time. We present a numerical model that predicts how these terraces develop under different climates and rates of rock uplift. Model results imply that measurements of long-term river incision are most susceptible to temporal bias in regions experiencing highly variable paleo-climate and slow rock uplift. Our model helps us make better measurements of river erosion and understand how climate and rock uplift shape landscapes.

1. Introduction

Strath terraces are surfaces that are laterally planed by river processes and abandoned when the rivers incise vertically into bedrock (Schanz et al., 2018). These landforms preserve valuable records of river incision (Craddock et al., 2010; Malatesta & Avouac, 2018; Rittenour, 2008; Stock et al., 2005; Zondervan et al., 2022), tectonic forcing (Bender et al., 2016; Wegmann & Pazzaglia, 2002a; Yanites et al., 2010a, 2010b) and climate change (Gran et al., 2013; Pan et al., 2003). Studies of river incision commonly use depositional ages of fluvial sediments capping strath terraces and elevation above the modern channel to calculate rates of incision. These measurements can, however, be influenced by a bias in which younger landforms may yield spurious higher incision rates (Finnegan et al., 2014; Gardner et al., 1987). The strength of these biases varies widely in landscapes worldwide (Nativ & Turowski, 2020). The observed biases have been explained by a combination of the long-tailed distribution of incision hiatuses (Finnegan et al., 2014) and the use of a dynamic channel elevation as a reference frame (Gallen et al., 2015). Yet, the importance of the incision hiatus or reference frame biases and their dependence on climate and tectonics is unconstrained.

Strath terraces are formed by a lateral planation process, that is often accentuated by sediment cover, followed by vertical incision either due to removal of a sediment cover or through bedrock meander cutoffs (Finnegan & Dietrich, 2011; Hancock & Anderson, 2002). In Figure 1, we show a schematic representation of the cyclical aggradation, planation, and abandonment common in some landscapes. During periods of low transport capacity (relative to sediment supply), sediment covers bedrock and slows or stops vertical bedrock erosion. During these periods, at-a-station channel elevation increases at the rate of rock uplift. While this is occurring, channels laterally plane broad bedrock surfaces known as straths. When climate shifts to a higher relative transport capacity (or decreases sediment supply relative to water discharge), sediment transport rates increase, and channels resume vertically eroding bedrock, abandoning strath terraces. In some regions, such cyclicity can be driven by glacial-

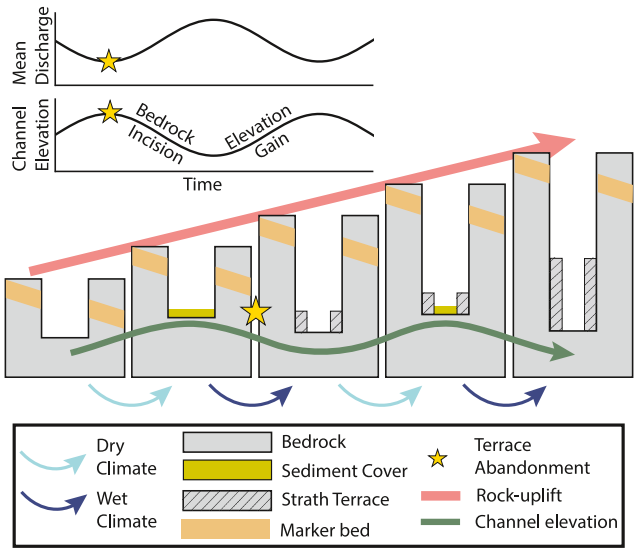

Figure 1. Mechanistic understanding of terrace genesis due to aggradation/incision cycles. During periods of dry climate, rivers receive less water thus their capacity to transport sediment and incise bedrock is decreased. Sediment aggrades further shielding bedrock from erosion during these periods. As rock uplift is constant through time in our modeling framework, the elevation of the bedrock channel increases when bedrock is shielded from erosion. Although we do not explicitly model lateral channel motion, we assume that during these periods of aggradation the channel moves laterally and planes off a strath. When the climate shifts from dry to wet, sediment transport rates increase, aggraded sediment is removed, and rivers resume bedrock incision. At these shifts is when we predict strath terraces to be abandoned. Repeated climate cycles after terrace abandonment increase the height of strath terraces. Through time, the local elevation of the bedrock channel is cyclical in response to these climate cycles (green line).

interglacial cycles (Pan et al., 2003), while in other regions, these cycles can be driven by regional climate variation (Breda et al., 2021; Wang et al., 2017; Zondervan et al., 2022).

Here we present a numerical model of 1-D bedrock river evolution which captures episodic aggradation and river incision, terrace abandonment, and incision hiatuses of rainfall-dominated drainage basins. Our model accounts for the impacts of both weather (10^{-2} yr discharge variability) and climate (10^{4} yr changes in mean state) while incorporating stochastic water discharge, stochastic sediment supply, and a dynamic channel width (DeLisle & Yanites, 2023). We evolve our model to equilibrium (minimal elevation changes) when averaged over 10^{6} model years and document terrace preservation, reproducing measurement biases in rates of river incision. We test our model under parameter space representing different climate and tectonic regimes and find that the bias is strongest when rock uplift is slow and climate is highly variable.

2. Model Mechanics

2.1. Overview

We model the evolution of channel bed elevation and incorporate impacts of stochastic water discharge, stochastic hillslope sediment supply, channel width changes, and vertical bedrock erosion (DeLisle & Yanites, 2023; Yanites, 2018). While the model is a 1-D river profile, periods of increased sedimentation and erosional hiatus are assumed to promote the planation processes through either valley widening (Hancock & Anderson, 2002) or bedrock meandering (Finnegan & Dietrich, 2011), leading to strath terrace formation. We investigate the impact of climate on our model by varying mean discharge through time; mean river discharge varies following an imposed sinusoid with a period which we vary from 20 Kyr to 120 Kyr. To capture differences in climate oscillation strength, we vary the amplitude of the variation from 10% to 60%. At a given timestep (2 weeks) in our model, we draw nondimensional water discharge from an inverse gamma distribution (representing stochastic weather events) and scale this discharge by the long-term mean discharge (representing long-timescale climate patterns). Note in the model, sediment supply is not constant but changes at each timestep depending on the water discharge (DeLisle & Yanites, 2023). Model parameters are described in the next sections.

2.2. Channel Elevation and Bedrock Erosion

The elevation ($z_{channel}$) of each node in our model river evolves from the competition between rock uplift (U_r) and bedrock erosion (E)

$$\frac{\partial z_{channel}}{\partial t} = \begin{cases} U_r - E & when\ h = 0 \\ U_r + \frac{\partial h}{\partial t} & when\ h > 0 \end{cases} \quad (1)$$

where h is the thickness of bedload sediment overlying bedrock in each model node. Uplift (U_r) is assumed to be steady and uniform over the course of a model simulation. Bedrock incision is modeled using a modified stream power law which accounts for the cover effect of immobile sediment.

$$E = FK\tau_b^a \quad (2)$$

Here, K is rock erodibility, a is a constant equal to 1 (Whipple et al., 2000), τ_b is basal shear stress, and F is fractional bedrock exposure which varies from zero (a bed fully buried by sediment) to 1 (a channel with fully exposed bedrock) and depends on the ratio of sediment supply to transport capacity (Sklar & Dietrich, 2004).

2.3. Stochastic Water Discharge

We model stochastic river discharge with a modified inverse gamma distribution of nondimensional daily water discharge (Qw^*). We chose this distribution as it captures the rarity of both extreme low and high discharge values, can easily be tuned to change river discharge variability, and has been used in many studies of the impact of discharge variability on bedrock channel evolution and morphology (Crave & Davy, 2001; DiBiase & Whipple, 2011; Lague et al., 2005). The continuous probability distribution of nondimensional daily discharge is:

$$PDF_{\overline{Qw},k_v}(Qw^*) = \frac{k_v^{\,k_v+1}}{\Gamma(k_v+1)} exp\left(-\frac{k_v}{Qw^*}\right) Qw^{*-(2+k_v)} dQw^* \quad (3)$$

where k_v controls discharge variability. For all models presented here we use $k_v = 0.3$, but this parameter can be calibrated with river gauging data. Qw^* is dimensionalized by scaling with the mean water discharge ($\overline{\overline{Qw}}(t)$) which changes over time with the imposed climate oscillation.

2.4. Sediment Supply

The rate of rock uplift controls the long-term average bedload sediment supply rate to a landscape (assumed to be 30% of total sediment load (Turowski et al., 2010)); however, bedload sediment supply from hillslopes to rivers is temporally variable. This is especially true in steep, tectonically active landscapes where landslides are prevalent (Campforts et al., 2022; Marc et al., 2019). To capture this, we vary sediment supply linearly with flood frequency (DeLisle & Yanites, 2023). Nondimensional sediment (Qs^*) delivery scales linearly with nondimensional river discharge (Equation 3). So that

$$Qs* = Qw* \quad (4)$$

We use nondimensional discharge, which represents the probability of an event of a given magnitude, rather than mean river discharge, to isolate the impact of climate on the capacity of rivers to move sediment and erode rock without varying long-term averaged sediment supply from hillslopes to channels. In our framework, a 100-year flood is always accompanied by the same volume of sediment, irrespective of whether climate is in a wet or dry period. This approach ensures that sediment supply is equal to the upstream rock uplift rate over geomorphically relevant timescales, regardless of current climate state or recent rate of river incision (e.g., Yanites, 2018).

2.5. Climate

We impose a sinusoidal oscillation in mean river discharge with periods that varies from 20 to 120 kyr in 20 kyr increments. For each period, we model amplitudes from 10% to 60% of mean river discharge in 10% increments. For example, if long-term average discharge at a node is equal to 100 m^3/s and we impose a climate magnitude of 40%, mean discharge is equal to 60 m^3/s during dry periods and 140 m^3/s during wet periods.

2.6. Numerical Experiments

We vary rock uplift rates from 0.5 mm/yr to 5 mm/yr and allow our model rivers to evolve to equilibrium under periodic climate forcing, and then undergo repeated climate cycles once dynamic equilibrium is attained. We document terrace abandonments, measure rates of river incision over the lifespan of a single terrace, and show trends in age-elevation relationships and measured incision rates across flights of inset terraces. The profiles are 100 km long and results are presented for the mid-point of the profile (50 km).

3. Mechanistic Drivers of Incision Biases

Figure 2 illustrates how the model captures the cycle of terrace formation through periods of sediment aggradation and incision (rock uplift of 0.5 mm/yr and 80Kyr period at 40% for the illustrated model run). Figure 2a is a time series of river discharge at the mid-point node in the modeled river. The pink line shows climate cycles in which mean discharge varies by ±40% relative to the long-term mean. The scatter around this line results from stochastic weather events.

10.1029/2024GL109339

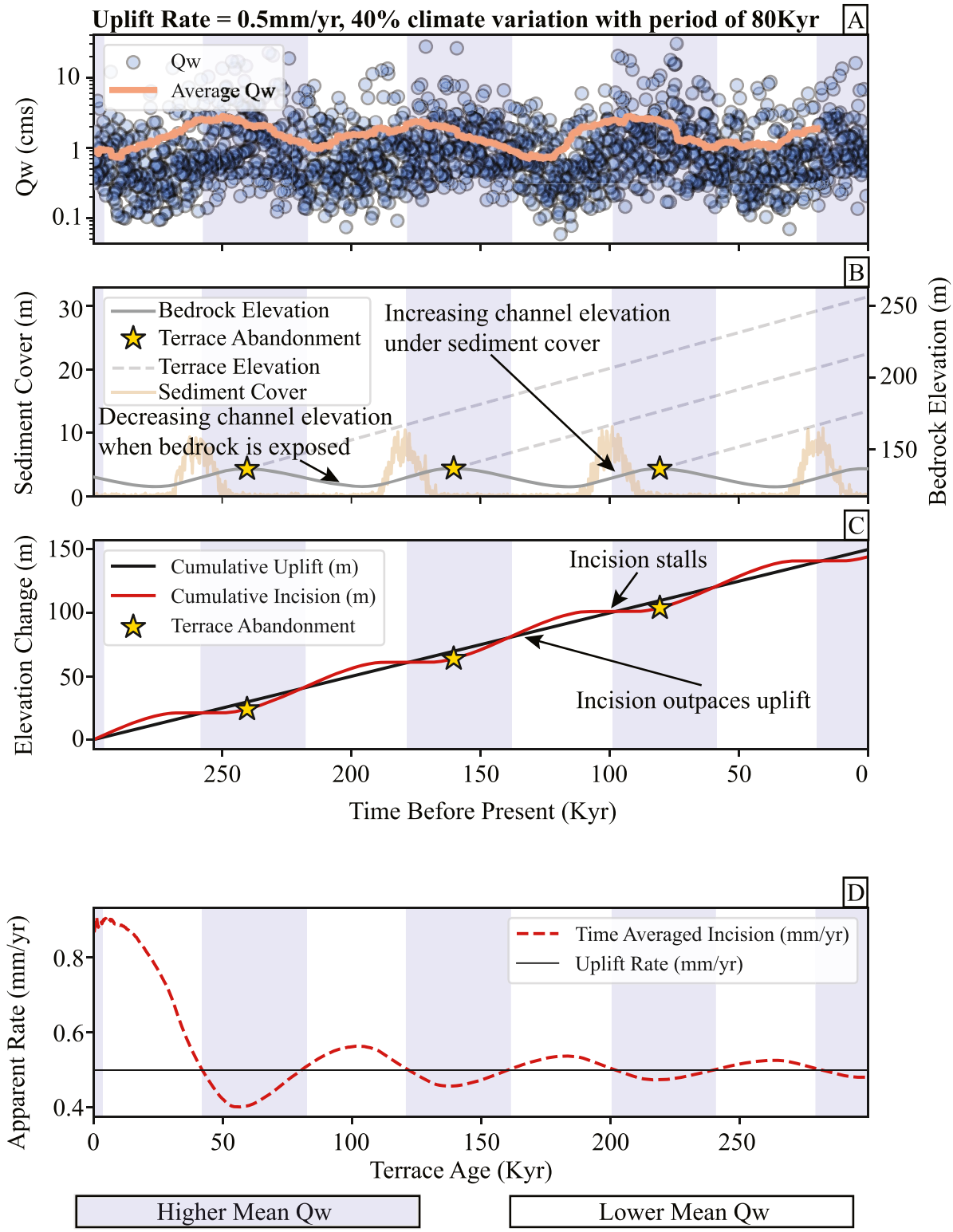

Figure 2. Time series of river discharge, channel morphology, and river incision during the development of a flight of strath terraces. All panels are colored to show times when climate (mean Q_w) is increasing and decreasing. (a) River discharge at one model node. Blue dots are stochastic discharge events, and the line is a moving average of river discharge. (b) Time series of channel elevation and sediment cover. Dashed lines project terrace elevation following abandonment at yellow stars. (c) Cumulative rock uplift and incision. Terraces are abandoned at times marked by yellow stars. (d) Measurements of river incision through time for one uplifting strath terrace.

Figure 2b shows a time series of bedrock elevation and sediment cover at a node in our model river. We observe decreasing channel elevations relative to an unmoving datum during periods of wet climate, when sediment transport and bedrock erosion is elevated. Conversely, we see bedrock elevations increase when the climate is drier, as decreases in sediment transport capacity drive sediment aggradation which shields bedrock from mechanical weathering processes and allows rock uplift to outpace bedrock erosion. While not explicitly modeled, it is during these periods that lateral channel motion, not channel width changes, plane off a wide strath surface that gets abandoned during wetter climates.

Figure 2c plots cumulative rock uplift versus cumulative incision. Cumulative incision increases quickly during wet climates, and stalls when sediment aggradation is high during dry climates. We predict the time at which terraces are abandoned by locating the local minima in cumulative incision detrended by cumulative rock uplift (denote with yellow stars in Figures 2b and 2ure 2c). We chose this metric because incision rate increases quickly after these local minima, and we suggest this as the time at which a river resumes bedrock incision and abandons a terrace. The elevation of these terraces is projected forward in time (gray dashed lines) at the rate of rock uplift (Figure 2b). The intercepts of these lines with the *y*-axis represent final terrace elevations.

Figure 2d shows the time series of incision rate that would be measured for a single terrace as it uplifts relative to an unmoving reference elevation (we use the channel elevation at the time of terrace abandonment). Here we document the incision hiatus bias, in which the measured rate of river incision decreases with terrace age, even with a stationary reference frame (Finnegan et al., 2014; Sadler, 1981; Schumer & Jerolmack, 2009). We note that, depending on the elevation of the reference frame, the rate could eventually overcorrect and underpredict incision rates, oscillating and dampening around the rate of rock-uplift with time.

4. Model Terrace Flights

To document the presence of, and investigate controls on, the dynamic reference frame bias, we preserved flights of strath terraces over 250 k model years at dynamic equilibrium for models across our parameter space. We show results from one such flight of terraces (Figure 3), where model parameters are the same as those described for Figure 2. Terrace elevations are calculated by projecting elevation growth at the rate of rock uplift once the terrace is abandoned (Figure 2).

We plot terrace ages versus terrace heights (Figure 3a). Terrace height is measured as the difference between the final terrace elevation and either the channel elevation at the time of terrace abandonment (gray points and line), the long-term mean channel elevation (dark green points and line), or the fifth percentile value of channel elevation (light green points and line). These elevations are the elevation of the bedrock channel at a single node, which changes through time even at equilibrium in response to climate cycles (Figure 2b). We fit log-linear trends to flights of terraces using each method of terrace height measurement and report the slopes of these lines, normalized by the rate of rock uplift, (β) in Figure 3a.

The gray points preserve the true rate of rock uplift and river incision following terrace abandonment, and so the slope of this line is equal to the rate of rock uplift ($\beta = 1.0$). The dark green points and lines measure final terrace elevation above the long-term mean channel elevation which is lower than the channel elevation at the time of terrace abandonment, which occurs at local maxima in channel elevation (Figure 2b). This imparts a dynamic reference frame bias on our data, as the difference between mean channel elevation and channel elevation at the time of terrace abandonment represents a larger fraction of total terrace height for younger terraces than older terraces (Gallen et al., 2015). As such, $\beta = 0.89$ when using mean channel elevation. Using the fifth percentile elevation value increases the strength of the bias, where ß = 0.81. Since aggradation is a dominant mechanism of channel elevation maxima, using sediment thicknesses above strath treads can help constrain the magnitude of such biases (e.g., (Bender et al., 2023)).

We also calculate bedrock incision rates using each reference elevation described above and show that measured incision rates are higher over short time windows and when using a lower reference elevation (Figure 3b). This helps to explain the ubiquity of the biases in field measurements of bedrock incision, because if measurements are taken above a river channel that is in a period of incision (i.e., a period with significant exposed bedrock), our model predicts that the current channel elevation is lower than the channel elevation at the time of terrace abandonment, which generally occurs during a period of moderate sediment aggradation (Figure 2b).

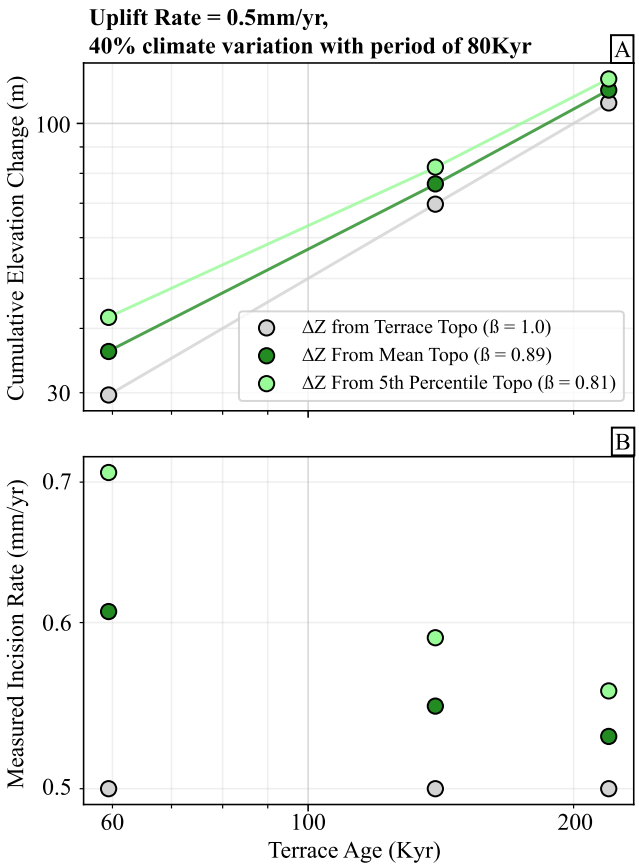

Figure 3. Documenting dynamic reference frame bias in a flight of model river terraces. (a) Terrace height versus. age measured relative to the channel elevation at the time of terrace abandonment, the mean channel elevation, and the fifth percentile channel elevation. (b) Rates of river incision for terraces of different ages measured using the symbols in panel (a).

5. Factors Controlling Bias Strength

We document the combined impact of rock uplift rate, climate oscillation magnitude, and climate period on the strength of the dynamic reference frame bias (Figure 4). Each point represents the slope of a line fit to terrace age versus cumulative elevation change measurements (e.g., Figure 3a). We use a reference frame that measures from the terrace elevation to the fifth percentile channel elevation (i.e., light green points in 3A) for all measurements. We test the impact of changing rock uplift rate and climate oscillation magnitude by plotting data from models that covary rock uplift from 0.5 mm/yr to 5 mm/yr, climate oscillation magnitude from 10% to 60% of long-term mean discharge, and climate period from 20 Kyr to 120 Kyr.

Figure 4a shows the ß values for models run with a moderate rock uplift rate of 0.5 mm/yr. Here we see that ß values decrease (biases are stronger) when climate variation is stronger and acts over longer time periods. The elevation of the bedrock channel, which we use as a reference frame for terrace height, is most variable in these scenarios with strongly varied climate over 120Kyr periods. Values of ß for this uplift rate range from 0.97 for a scenario with a 10% climate oscillation and a period of 20Kyr to 0.75 for a scenario with a 60% climate oscillation and a period of 120 Kyr. ß values for a fast uplift rate of 5 mm/yr document a similar trend (Figure 4b), where ß values are lowest with long-period and high-magnitude climate oscillation. Values of ß range from 0.89 to 0.99 for fast-uplifting models.

Our model predicts that dynamic reference frame biases in measurements of bedrock river incision rates are the strongest when rock uplift is slow and, thus, that measurements are more reliable in fast-uplifting landscapes. This occurs because terrace elevation above the active channel increases at the rock uplift rate once terraces are abandoned. In fast-uplifting landscapes, terraces quickly become tall, and so the measured terrace elevation is less impacted by the dynamic elevation of the channel. In the slower uplifting models, the variability in channel elevation accounts for a larger fraction of total terrace height and thus imparts a stronger bias on measured incision rates.

6. Discussion

In this study, we present a numerical model that predicts the strength of measurement biases in rates of river incision by accounting for bedrock incision, sediment delivery and transport, tectonic rock uplift, and both weather and climate. Our model expands on conceptual models (Gallen et al., 2015), numerical models (Hancock & Anderson, 2002), and field observations (Finnegan et al., 2014; Gardner et al., 1987; Nativ & Turowski, 2020) and allows for interrogation of individual variables on the strength of these biases. This model is an important step toward understanding this widespread but enigmatic complicating factor in studies using rates of river incision from strath terraces. For example, with parameterization representative of the tectonics and regional climate history of a region, one could quantify potential biases in tectonic rock-uplift rates inferred from measured rates of river incision. As river incision if often one of the only markers of rock-uplift at 10^3–10^5 yr timescales, such biases are critical to improving uncertainty quantification.

The dependence on rock-uplift also suggests that the bias may also be strongly influenced by rock erodibility. To explore this potential sensitivity, we reran a select few models with a 3x increase and decrease in K. We calculate a 5%–10% decrease in β (increased bias) for the higher erodibility (weaker rock) runs, while a 5%–10% increase in β (less bias) for the lower erodibility (stronger rock). We interpret this as a sensitivity of the system to sediment supply variability. With harder rock, the baseline system is steeper relative to the softer rock, and thus less sensitivity to sediment cover-induced hiatus. This means, the system spends less time with slow or zero vertical incision, shorting the hiatus duration, and thus lowering the calculated bias.

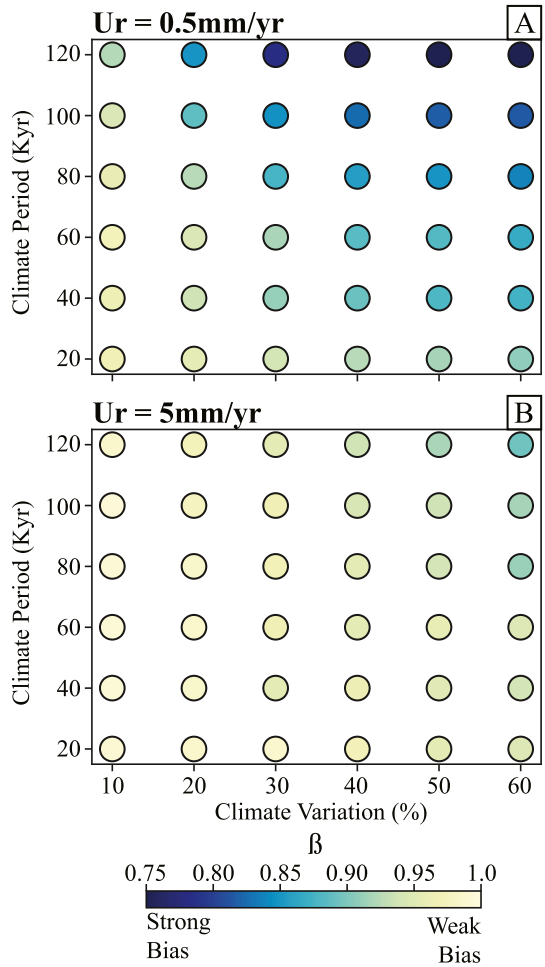

Figure 4. Relationships between magnitude of climate variation, climate variation period, and rate of rock uplift, strength of dynamic reference frame bias (ß). Lower values of ß occur when measured incision rate bias with measurement window is stronger. (a) Results for Ur = 0.5 mm/yr. (b) Results for Ur = 5 mm/yr. For both uplift rates, biases are strongest (ß values are lower) for longer and stronger climate oscillations. Biases are stronger under moderate rock uplift (5 mm/yr) than fast rock uplift (5 mm/yr).

Many modeling parameters that are important in controlling the dynamics of evolving bedrock rivers have been held constant across the model runs presented here to isolate the impact of climate variation on river incision measurement biases. Factors such as rock erodibility and grain size influence the slope of bedrock rivers, and variations in these parameters may yield different calculated values of ß as a result. Our dynamic width algorithm (Yanites, 2018) can be modified to allow for greater variations in channel width during periods of aggradation and incision. We refer the reader to Yanites (2018) for documentation of different bedrock incision rules (e.g., saltation-abrasion) within this modeling framework. While we vary the magnitude and period of our sinusoidal climate oscillation, we acknowledge that a simple sine wave is a simplified representation of real-world climate variations. While these parameters should be explored during efforts to calibrate our model to specific landscapes, we keep them constant for the purposes of this exploratory modeling study, and we do not believe that modifying them would detract from overall trends observed between rock uplift, climate oscillation, and the strength of measurement biases in rates of river incision.

The modeling framework presented in this paper links sediment delivery linearly with river discharge. We vary only river discharge over climate scales and not sediment supply to isolate the ability of a river to transport sediment and erode bedrock during repeated climate cycles, but we recognize that the relationships between climate change and sediment dynamics are complex and not well understood (Malatesta & Avouac, 2018). Future work should aim to disentangle these factors and improve our understanding of the effects of changes in long-term sediment supply which may overprint the effects described here.

Our model predicts terrace abandonment, marked by periods of increased vertical bedrock incision, which occurs when climates transition from dry (lower relative transport capacity) to wet (higher relative transport capacity); this is driven by an increase in capacity for both sediment transport and bedrock erosion due to higher bed shear stresses. Global datasets (Schanz et al., 2018) show, however, that the conditions that lead to strath planation and abandonment are diverse and variable. While we account for only one such mechanism here, many other factors such as long-term averaged sediment supply, rock uplift rate, and discharge variability are readily modified in our modeling framework and thus it could be used to examine a variety of mechanisms for terrace genesis.

The range of ß values that we predict using our modeling framework (from 0.75 to 0.99) is smaller than the range of ß values observed in global compilations, which range from <0.5 to >1.0 (Finnegan et al., 2014; Nativ & Turowski, 2020). There are two possible explanations for this mismatch. First, our model may underpredict the strength of biases because of the unchanging nature of sediment supply in response to climate shifts within our modeling framework. While we made this decision intentionally to isolate the impact of river discharge and capacity for sediment transport and erosion, further investigation of model predictions where sediment supply is modulated by climate shifts alongside changes in river discharge may broaden the range of predicted ß values. Second, we present results from terraces that form while the model is in dynamic equilibrium. Global compilations of these biases may include landscapes in which local tectonics are transient, which would impart a stronger bias (lower ß values) than the ones we predict here.

Strath terraces are often used as markers of climate change in net erosional landscapes (Molnar et al., 1994; Tao et al., 2020; Wegmann & Pazzaglia, 2002b), and inset strath terrace suites represent some of the best archives of past climates. However, understanding how terrace genesis results from combined climate, tectonic, and fluvial forces is critical to accurately interpreting climatic signals from terraces. Our model presents a significant step

toward a better understanding of these systems. River discharge, drainage area, sediment supply, tectonic uplift, rock strength, and grain size can all be modified in our modeling framework to capture characteristics specific to a single landscape. Through thoughtful selection of these variables and exploration of uncertainties in climatic and geomorphic forcings, our model could be used to improve confidence in interpreting climatic forcings in the formation of strath terraces.

7. Conclusions

Our numerical modeling framework predicts strath terrace development, including hiatus and reference frame bias, as a function of the combined impact of fluvial mechanics, tectonics, weather, and climate. We find that measurement biases in rates of river incision are driven by the combined forcing of tectonic rock uplift and climate oscillations, which modulate the relative rates of sediment supply and capacity. These biases are strongest when rock uplift is slow, and climate is highly variable over long time periods, leading to extensive hiatuses in vertical incision. Our work builds a new framework that will allow better linkages between field observations of river incision and terrace evolution with predictive numerical models of landscape evolution. The model increases the reliability of measurements of river incision by providing a path toward direct correcting for incision rate biases and can be applied in studies that aim to reconstruct climate histories from current landscape form.

Data Availability Statement

The OTTERpy code used for this study is available via MIT License and developed openly at https://github.com/clarkedelisle/OTTERPy (Yanites, 2024b). Input files and modifications to the OTTERpy code needed to reproduce the model runs and figures contained in the manuscript is available via Zenodo (Yanites, 2024a).

Acknowledgments
CD was supported by NSF EAR-1727736 and the Department of Defense National Science and Engineering Graduate Fellowship. BJY was supported by NSF EAR-2123412 and NSF EAR-2120211.

References

Bender, A. M., Amos, C. B., Bierman, P., Rood, D. H., Staisch, L., Kelsey, H., & Sherrod, B. (2016). Differential uplift and incision of the Yakima River terraces, central Washington State. *Journal of Geophysical Research: Solid Earth*, *121*(1), 365–384. https://doi.org/10.1002/2015JB012303

Bender, A. M., Lease, R. O., Rittenour, T., & Jones, J. V. (2023). Rapid active thrust faulting at the northern Alaska Range front. *Geology*, *51*(6), 527–531. https://doi.org/10.1130/G51049.1

Breda, C., do Nascimento Pupim, F., Sawakuchi, A. O., & Mineli, T. D. (2021). The role of bedrock and climate for the Late Quaternary erosive-depositional behavior of an intraplate tropical river: The Tietê River case, southeastern Brazil. *Geomorphology*, *389*, 107834. https://doi.org/10.1016/j.geomorph.2021.107834

Campforts, B., Shobe, C. M., Overeem, I., & Tucker, G. E. (2022). The Art of landslides: How stochastic mass wasting shapes topography and influences landscape dynamics. *Journal of Geophysical Research: Earth Surface*, *127*(8), e2022JF006745. https://doi.org/10.1029/2022JF006745

Craddock, W. H., Kirby, E., Harkins, N. W., Zhang, H., Shi, X., & Liu, J. (2010). Rapid fluvial incision along the Yellow River during headward basin integration. *Nature Geoscience*, *3*(3), 209–213. https://doi.org/10.1038/ngeo777

Crave, A., & Davy, P. (2001). A stochastic "precipiton" model for simulating erosion/sedimentation dynamics. *Computers & Geosciences*, *27*(7), 815–827. https://doi.org/10.1016/S0098-3004(00)00167-9

DeLisle, C., & Yanites, B. J. (2023). Rethinking variability in bedrock rivers: Sensitivity of hillslope sediment supply to precipitation events modulates bedrock incision during floods. *Journal of Geophysical Research: Earth Surface*, *128*(9), e2023JF007148. https://doi.org/10.1029/2023JF007148

DiBiase, R. A., & Whipple, K. X. (2011). The influence of erosion thresholds and runoff variability on the relationships among topography, climate, and erosion rate. *Journal of Geophysical Research*, *116*(F4), F04036. https://doi.org/10.1029/2011JF002095

Finnegan, N. J., & Dietrich, W. E. (2011). Episodic bedrock strath terrace formation due to meander migration and cutoff. *Geology*, *39*(2), 143–146. https://doi.org/10.1130/G31716.1

Finnegan, N. J., Schumer, R., & Finnegan, S. (2014). A signature of transience in bedrock river incision rates over timescales of 104-107 years. *Nature*, *505*(7483), 391–394. https://doi.org/10.1038/nature12913

Gallen, S. F., Pazzaglia, F. J., Wegmann, K. W., Pederson, J. L., & Gardner, T. W. (2015). The dynamic reference frame of rivers and apparent transience in incision rates. *Geology*, *43*(7), 623–626. https://doi.org/10.1130/G36692.1

Gardner, T. W., Jorgensen, D. W., Shuman, C., & Lemieux, C. R. (1987). Geomorphic and tectonic process rates: Effects of measured time interval. *Geology*, *15*(3), 259–261. https://doi.org/10.1130/0091-7613(1987)15<259:gatpre>2.0.co;2

Gran, K. B., Finnegan, N., Johnson, A. L., Belmont, P., Wittkop, C., & Rittenour, T. (2013). Landscape evolution, valley excavation, and terrace development following abrupt postglacial base-level fall. *GSA Bulletin*, *125*(11–12), 1851–1864. https://doi.org/10.1130/B30772.1

Hancock, G. S., & Anderson, R. S. (2002). Numerical modeling of fluvial strath-terrace formation in response to oscillating climate. *Geological Society of America Bulletin*, *114*(9), 1131–1142. https://doi.org/10.1130/0016-7606(2002)114<1131:nmofst>2.0.co;2

Lague, D., Hovius, N., & Davy, P. (2005). Discharge, discharge variability, and the bedrock channel profile. *Journal of Geophysical Research*, *110*(F4). https://doi.org/10.1029/2004JF000259

Malatesta, L. C., & Avouac, J.-P. (2018). Contrasting river incision in north and south Tian Shan piedmonts due to variable glacial imprint in mountain valleys. *Geology*, *46*(7), 659–662. https://doi.org/10.1130/G40320.1

Marc, O., Behling, R., Andermann, C., Turowski, J. M., Illien, L., Roessner, S., & Hovius, N. (2019). Long-term erosion of the Nepal Himalayas by bedrock landsliding: The role of monsoons, earthquakes and giant landslides. *Earth Surface Dynamics*, *7*(1), 107–128. https://doi.org/10.5194/esurf-7-107-2019

Molnar, P., Erik, T. B., Burchfiel, B. C., Deng, Q., Feng, X., Li, J., et al. (1994). Quaternary climate change and the formation of river terraces across growing anticlines on the north Flank of the Tien Shan, China. *The Journal of Geology*, *102*(5), 583–602. https://doi.org/10.1086/629700

Nativ, R., & Turowski, J. M. (2020). Site dependence of fluvial incision rate scaling with timescale. *Journal of Geophysical Research: Earth Surface*, *125*(11), e2020JF005808. https://doi.org/10.1029/2020JF005808

Pan, B., Burbank, D., Wang, Y., Wu, G., Li, J., & Guan, Q. (2003). A 900 k.y. record of strath terrace formation during glacial-interglacial transitions in northwest China. *Geology*, *31*(11), 957–960. https://doi.org/10.1130/G19685.1

Rittenour, T. M. (2008). Luminescence dating of fluvial deposits: Applications to geomorphic, palaeoseismic and archaeological research. *Boreas*, *37*(4), 613–635. https://doi.org/10.1111/j.1502-3885.2008.00056.x

Sadler, P. M. (1981). Sediment accumulation rates and the completeness of stratigraphic sections. *The Journal of Geology*, *89*(5), 569–584. https://doi.org/10.1086/628623

Schanz, S. A., Montgomery, D. R., Collins, B. D., & Duvall, A. R. (2018). Multiple paths to straths: A review and reassessment of terrace genesis. *Geomorphology*, *312*, 12–23. https://doi.org/10.1016/j.geomorph.2018.03.028

Schumer, R., & Jerolmack, D. J. (2009). Real and apparent changes in sediment deposition rates through time. *Journal of Geophysical Research*, *114*(F3), 12. https://doi.org/10.1029/2009JF001266

Sklar, L. S., & Dietrich, W. E. (2004). A mechanistic model for river incision into bedrock by saltating bed load. *Water Resources Research*, *40*(6), n/a-n–a. https://doi.org/10.1029/2003WR002496

Stock, J. D., Montgomery, D. R., Collins, B. D., Dietrich, W. E., & Sklar, L. (2005). Field measurements of incision rates following bedrock exposure: Implications for process controls on the long profiles of valleys cut by rivers and debris flows. *Geological Society of America Bulletin*, *117*(1–2), 174–194. https://doi.org/10.1130/B25560.1

Tao, Y., Xiong, J., Zhang, H., Chang, H., & Li, L. (2020). Climate-driven formation of fluvial terraces across the Tibetan plateau since 200 ka: A review. *Quaternary Science Reviews*, *237*, 106303. https://doi.org/10.1016/j.quascirev.2020.106303

Turowski, J. M., Rickenmann, D., & Dadson, S. J. (2010). The partitioning of the total sediment load of a river into suspended load and bedload: A review of empirical data. *Sedimentology*, *57*(4), 1126–1146. https://doi.org/10.1111/j.1365-3091.2009.01140.x

Wang, Z., Meyer, M. C., Gliganic, L. A., Hoffmann, D. L., & May, J.-H. (2017). Timing of fluvial terrace formation and concomitant travertine deposition in the upper Sutlej River (Tirthapuri, southwestern Tibet) and paleoclimatic implications. *Quaternary Science Reviews*, *169*, 357–377. https://doi.org/10.1016/j.quascirev.2017.06.009

Wegmann, K. W., & Pazzaglia, F. J. (2002a). Holocene strath terraces, climate change, and active tectonics: The Clearwater River basin, Olympic Peninsula, Washington State. *Geological Society of America Bulletin*, *114*(6), 731–744. https://doi.org/10.1130/0016-7606(2002)114<0731:hstcca>2.0.co;2

Wegmann, K. W., & Pazzaglia, F. J. (2002b). Holocene strath terraces, climate change, and active tectonics: The Clearwater River basin, Olympic Peninsula, Washington State. *Geological Society of America Bulletin*, *114*(6), 731–744. https://doi.org/10.1130/0016-7606(2002)114<0731:hstcca>2.0.co;2

Whipple, K. X., Hancock, G. S., & Anderson, R. S. (2000). River incision into bedrock: Mechanics and relative efficacy of plucking, abrasion, and cavitation. *Geological Society of America Bulletin*, *112*(3), 490–503. https://doi.org/10.1130/0016-7606(2000)112<0490:riibma>2.3.co;2

Yanites, B. (2024a). Modeling climate and tectonic controls on bias in measured River Incision rates. [Dataset]. *Zenodo*. https://doi.org/10.5281/zenodo.13693846

Yanites, B. (2024b). byanites/OTTERPy: v1.3 (Version v1.3.0) Software. *Zenodo*. https://doi.org/10.5281/zenodo.13695611

Yanites, B. J. (2018). The dynamics of channel slope, width, and sediment in actively eroding bedrock river systems. *Journal of Geophysical Research: Earth Surface*, *123*(7), 1504–1527. https://doi.org/10.1029/2017JF004405

Yanites, B. J., Tucker, G., Mueller, K., Chen, Y., Wilcox, T., Huang, S., & Shi, K. (2010a). Incision and channel morphology across active structures along the Peikang River, central Taiwan: Implications for the importance of channel width. *Geological Society of America Bulletin*, *122*(7–8), 1192–1208. https://doi.org/10.1130/B30035.1

Yanites, B. J., Tucker, G. E., Mueller, K. J., & Chen, Y.-G. (2010b). How rivers react to large earthquakes: Evidence from central Taiwan. *Geology*, *38*(7), 639–642. https://doi.org/10.1130/G30883.1

Zondervan, J. R., Stokes, M., Telfer, M. W., Boulton, S. J., Mather, A. E., Buylaert, J.-P., et al. (2022). Constraining a model of punctuated river incision for Quaternary strath terrace formation. *Geomorphology*, *414*, 108396. https://doi.org/10.1016/j.geomorph.2022.108396